

Fabrication of Magnetic and EMI Shielding Wood-Based Composite by Electroless Ni-Fe-P Plating Process

Li Wang, Changhong Shi, and Lijuan Wang*

A Ni-Fe-P alloy coating was applied to *Triplochiton scleroxylon* veneers to prepare a magnetic, corrosion-resistant, electromagnetism-shielding wood-based composite. The effects of solution pH on metal deposition, surface resistivity, crystal structure, and the chemical composition of the coatings were investigated. The electro-conductivity, anti-corrosion properties, and magnetic and electromagnetic shielding performances were also measured. The results showed that increasing the pH favored the co-deposition of nickel and iron; metal deposition increased and surface resistivity decreased. The Ni-Fe-P alloy coatings obtained at pH values between 8.8 and 9.6 were all crystalline. VSM data revealed that the addition of elemental Fe to the deposits remarkably increased the magnetic properties of the products. The anti-corrosion properties of Ni-Fe-P coatings were higher than those of Ni-P coatings prepared in 3.5 wt.% NaCl solution. The electromagnetic shielding effectiveness value of Ni-Fe-P plated veneer reached 45 to 60 dB at frequencies ranging from 9 kHz to 1.5 GHz.

Keywords: *Triplochiton scleroxylon*; *Electroless Ni-Fe-P plating*; *Magnetic*; *Corrosion resistance*; *Electromagnetic shielding effectiveness*

Contact information: Key Laboratory of Bio-based Material Science and Technology of Ministry of Education, Northeast Forestry University, 26 Hexing Road, Harbin 150040, P. R. China;

* *Corresponding author:* donglinwlj@163.com

INTRODUCTION

In recent years, extensive development of various electronic devices and systems has caused serious electromagnetic interference (EMI) issues (Lee *et al.* 2006). Effective EMI shielding materials are required for a wide variety of applications (Al-Saleh and Sundararaj 2009; Kim *et al.* 2011). Wood-based EMI shielding composites have the advantages of being relatively light weight, with low cost, and visual appeal. They are a good alternative to metal foil for some commercial applications. Electroless plating is an effective approach to prepare wood-based composites for EMI shielding by depositing metal or alloy coatings onto the wood surface. In the past two decades, researchers have focused on electroless plating nickel or copper coatings to the wood surface to create wood-based composites that are electrically conductive and provide EMI shielding. Nagasawa *et al.* (1990; 1991; 1992; 1999) confirmed in previous studies that particleboard treated with nickel-plated wood particles exhibit excellent antistatic and electromagnetic shielding performance. Wang *et al.* (2005; 2006a; 2006b; 2007; 2011) investigated the plating parameters of Ni-P alloy and copper coatings on wood veneers and analyzed the relationship between plating conditions and the chemical composition and structure of the coatings. They also studied coating activation methods and developed a simple activation process for the electroless plating of wood. However, the corrosion resistance of Ni-P and copper weakens in wet conditions. In order to obtain corrosion-

resistant wood-based composites, Hui *et al.* (2014) deposited a ternary Ni-Cu-P alloy onto wood veneers. It was found that Ni-Cu-P coatings had better corrosion resistance than Ni-P alloy or copper coatings. However, the ternary Ni-Cu-P alloy has poor magnetic performance. An *et al.* (2008) verified that the magnetic performance of Ni-Fe-P coatings is proportional to the amount of iron deposited with the coating. Wang *et al.* (2000) reported that the corrosion resistance of Ni-Fe-P coating applied on the surface of copper or carbon steel is high. Gao (2005) studied the formation mechanism of amorphous Ni-Fe-P coatings, which demonstrated that the amorphous structure is formed with centered phosphorus atoms enveloped by nickel and iron atoms. Ni-Fe-P coatings on substrates such as glass microspheres, copper, and carbon steel have also been studied. However, there have been no reports about electroless plating of Ni-Fe-P on the surface of wood.

Triplochiton scleroxylon is a fast-growing tree of tropical Africa. The wood is ring-porous and known as a low-quality obeche. In China, it is used as raw material to manufacture decorative laminated veneer. In order to confirm the universality of the simple activation process for various wood, in this work, Ni-Fe-P alloy coatings were deposited on *Triplochiton scleroxylon* veneers to prepare corrosion-resistant wood-based composites with magnetic and electromagnetic shielding functionalities. The effects of pH on the metal deposition, surface resistivity, crystal structure, and chemical composition of the coatings were investigated. The anti-corrosion properties, magnetic parameters, and electromagnetic shielding effectiveness were also measured.

EXPERIMENTAL

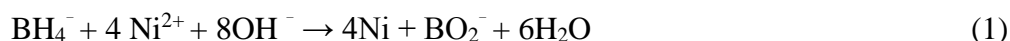
Materials

The substrates used in the experiments of this study were *Triplochiton scleroxylon* wood veneers. The samples used for surface resistivity studies were cut into squares of size 50×50 mm. The samples for magnetic studies were cut into squares of size 3×6 mm. All chemicals were of analytical grade and distilled water was used to prepare all solutions.

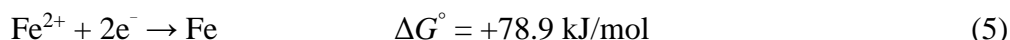
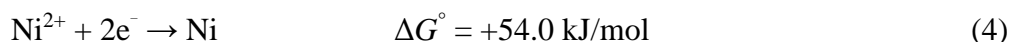
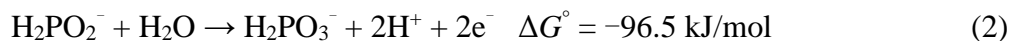
Activation and Plating Process

First, wood samples were dipped in KBH_4 solution at room temperature for long enough to load an adequate amount of KBH_4 onto their surface. Next, the veneers loaded with KBH_4 and NaOH were left in open air for 1 min and then put into the plating solution for 30 min to begin the activation process and complete the plating process in a single bath. The plated veneers were vigorously washed with tap water and dried to constant weight at 102 °C. The solution composition and the operation conditions of the electroless Ni-Fe-P plating are listed in Table 1. The pH was adjusted with $\text{NH}_3 \cdot \text{H}_2\text{O}$.

The reducing ability of KBH_4 is higher than that of H_2PO_2^- . Ni^{2+} in the plating solution first reacted with KBH_4 before reacting with H_2PO_2^- , which produced Ni^0 clusters on the wood surface which acted as catalytic centers to catalyze subsequent electroless plating. The reaction is as follows,



Under the catalytic action of Ni⁰ clusters, Ni²⁺ and Fe²⁺ react with H₂PO₂⁻ to form a Ni-Fe-P coating bound to the wood surface. The chemical reactions involved in this process are (Pang *et al.* 2012),



According to the standard ΔG° of each reaction, it is clear that Ni, Fe, and P can be reduced by sodium hypophosphite (NaH₂PO₂) and that the rate of reaction for Ni reduction is greater than that for Fe. In addition, phosphorus and hydrogen form as by-products. Deposited Ni and Fe atoms serve as self-catalytic centers for further nickel and iron deposition. Ni-Fe-P-coated wood veneers were obtained *via* this electroless plating process.

Table 1. Solution Composition and Operation Conditions for Electroless Ni-Fe-P Plating

Chemical	Concentration (g/L)
NiSO ₄ ·6H ₂ O	20 to 50
(NH ₄) ₂ Fe(SO ₄) ₂ ·6H ₂ O	10 to 30
NaH ₂ PO ₂ ·H ₂ O	20 to 40
KNaC ₄ H ₄ O ₆ ·4H ₂ O	40 to 80
(NH ₄) ₂ SO ₄	20 to 50
pH	8 to 10
Temperature	90 °C

Characterization Methods

The crystal structure of the coatings was analyzed by X-ray diffraction (XRD, model D/MAX-3B, Rigaku). The chemical composition of the coatings was determined by energy-dispersive X-ray analysis with an EDAX-falcon analyzer (EDS). A vibrating sample magnetometer (VSM, model SP-2100A, America LakeShore Company) was used to measure the hysteresis loop of samples at room temperature to determine the saturation magnetization.

Measurement of metal deposition

The wood veneers, before and after Ni-Fe-P coating, were dried to constant weights G_0 and G_1 , respectively. The metal deposition was calculated according to the formula,

$$\text{Metal deposition (mg/cm}^2\text{)} = (G_1 - G_0)/S \quad (6)$$

where S is the total surface area of the sample (cm²).

Surface resistivity measurement

The surface resistivity of the metallized veneers was evaluated with a YD2511A-type smart low direct-current resistance tester according to the Chinese National Military Standard GJB-2604-96. Because the structure of wood is anisotropic, the plated veneers were also anisotropic in electrical conductivity; the surface resistivity parallel to the fiber direction is not equal to that traverse the fiber direction. Thus, multiple points on the sample surface should be tested and Eq. 7 should be used to calculate the average surface resistivity,

$$R_s (\Omega/\text{cm}^2) = R/S \quad (7)$$

where R is the resistance value of the sample (Ω) and S is the area of the coating through which electrical current passes (cm^2).

Shielding effectiveness studies

The shielding effectiveness (SE) of the metallized veneers was evaluated using the Agilent E4402B spectrum analyzer and a standard butt coaxial cable line with a flange based on the Chinese Industrial Standard SJ20524-95. The equation used to calculate the SE value is as follows,

$$SE (\text{dB}) = -10 \times \lg (P_{out}/P_{in}) \quad (8)$$

where P_{out} and P_{in} are the incident and transmitted power, respectively.

Electrochemical corrosion analysis

The corrosion resistance of metallized veneers was measured with an LK2005A-type electrochemical work station. A standard three-electrode system was used to measure the polarization curve, in which the plated veneer was used as the working electrode and the saturated calomel electrode and platinum sheet acted as the reference electrode and auxiliary electrode, respectively. The corrosion tests were carried out in 3.5 wt.% NaCl solution to determine the corrosion potentials (E_{corr}), corrosion current densities (I_{corr}), and polarization resistances (R_p).

RESULTS AND DISCUSSION

Effects of pH on Chemical Composition of the Coatings

The pH is a key factor affecting the electroless plating of the Ni-Fe-P alloy. The effects of pH on the composition of deposits are shown in Fig. 1. As the pH increased from 8.8 to 9.4, the percentage of nickel in the deposits decreased from 93.40 to 92.69 wt.%, the phosphorus content in the deposits decreased from 2.23 to 1.80 wt.%, and the iron content increased from 4.37 to 5.51 wt.%. Increasing the pH further did not markedly change the composition of the plating. In alkaline medium, potential of hypophosphite negatively shifts so that its reduction ability increases. Therefore, with the increase of pH, hypophosphite reduce Fe^{2+} to Fe^0 more easily. Coactions between H_2PO_2^- and Fe^{2+} at high pH were more beneficial than those at lower pH, while the influence of solution pH on the reduction Ni^{2+} was not clear.

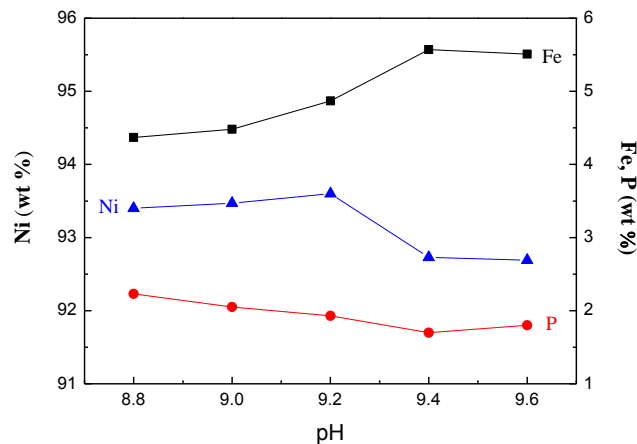


Fig. 1. Effect of solution pH on chemical composition of the coatings

Effects of pH on Crystal Structure of the Coatings

The effects of pH on the crystal structure of deposits are shown in Fig. 2. XRD analysis indicated a peak at a 2θ value of 22.56° , which is a characteristic peak of cellulose in the *Triplochiton scleroxylon* veneer. The sharp peaks at 2θ values of 44.36° , 51.53° , and 76.60° are attributed to Ni(111), Ni(200), and Ni(220), respectively, and illustrate the crystalline nature of the layer. This result is related to the low P content and the fact that there is little distortion of the crystalline structure of Ni-Fe by P atoms. All Ni-Fe-P alloy coatings obtained at pH from 8.8 to 9.6 were crystalline.

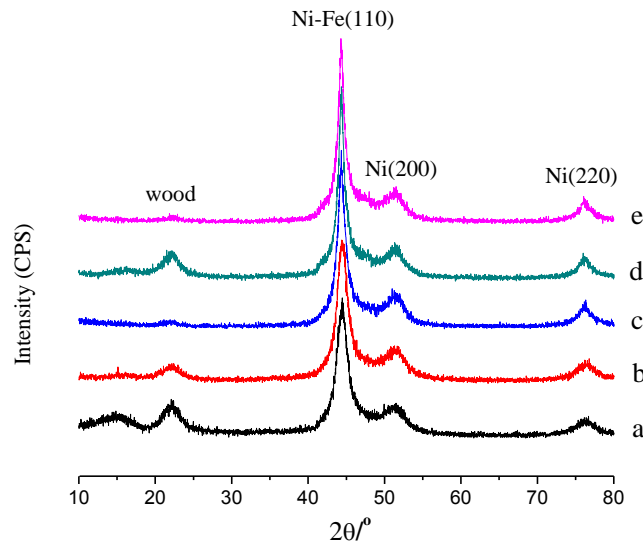


Fig. 2. XRD patterns of Ni-Fe-P coatings based on the pH value of the plating solution: (a) pH 8.8, (b) pH 9.0, (c) pH 9.2, (d) pH 9.4, and (e) pH 9.6 (temperature 85°C)

Effects of pH on Surface Resistivity and Metal Deposition of the Coatings

The effects of pH on the surface resistivity and metal deposition are shown in Fig. 3. As the pH was increased from 8.8 to 9.4, the surface resistivity decreased from 407.71 to $197.82\text{ m}\Omega/\text{cm}^2$ and the metal deposition increased from 10.32 to $12.04\text{ mg}/\text{cm}^2$.

However, as the pH was increased further to 9.6, the surface resistivity increased and metal deposition decreased. This is because excess OH^- combined with Ni^{2+} and Fe^{2+} , producing $\text{Ni}(\text{OH})_2$ and $\text{Fe}(\text{OH})_2$, making the solution unstable and the coatings rough. According to the plating solution experiments, a pH value of 9.4 was discovered to be optimal, yielding stable solutions and uniform deposits.

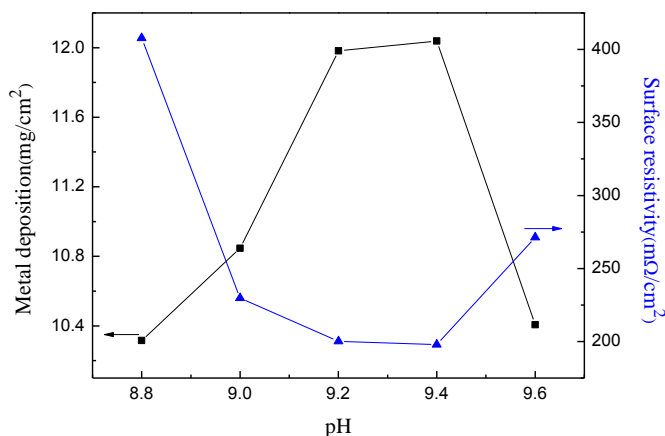


Fig. 3. Effect of solution pH on metal deposition and surface resistivity (temperature 85 °C)

Effects of the pH Value on the Morphology of the Coatings

The surface morphologies of Ni-Fe-P coatings under various pH are shown in Fig. 4. All coatings have the typical cellular morphology characteristics. At pH from 8.8 to 9.6, the coatings were uniform, smooth, and compact. The metal sheen was also obvious. The difference from morphologies of the coatings under various pH was not significant.

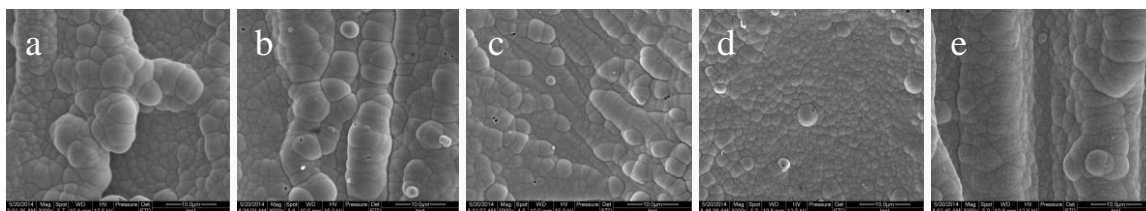


Fig. 4. SEM images of Ni-Fe-P-coating with varying solution pH value: (a) pH 8.8; (b) pH 9.0; (c) pH 9.2; (d) pH 9.4; (e) pH 9.6 (temperature 85 °C)

Shielding Effectiveness

The electromagnetic shielding results of the plated and raw wood are shown in Fig. 5. At frequencies ranging from 9 kHz to 1.5 GHz, the shielding effectiveness of the raw *Triplochiton scleroxylon* wood veneer was near zero, indicating that there was almost no shielding of electromagnetic waves. However, the shielding effectiveness value of plated wood veneers reached 45 to 60 dB. According to the relevant standards, the shielding effectiveness of electromagnetic shielding material generally must be at least 35 dB. Thus, the Ni-Fe-P-coated veneers meet some EMI shielding application requirements in the civil and military fields.

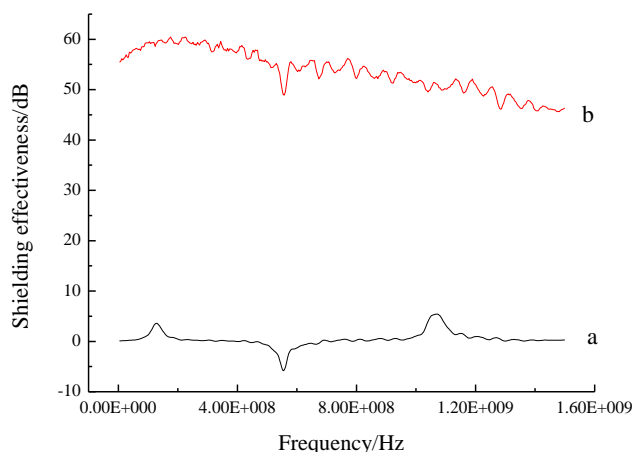


Fig. 5. Electromagnetic shielding effectiveness of the plated and raw wood veneers (a) pristine veneer, and (b) plated veneer (pH 9.4, temperature 90 °C)

Magnetic Analysis

The magnetic properties of the plated veneers were studied. The hysteresis loops acquired at room temperature are shown in Fig. 6.

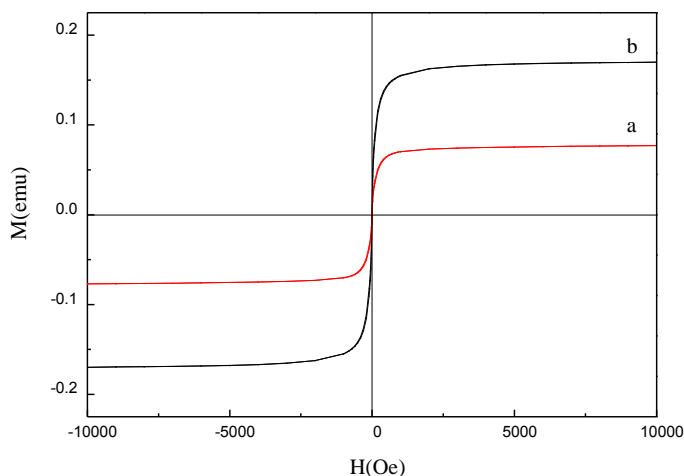


Fig. 6. Magnetic hysteresis loops of electroless Ni-Fe-P-plated veneers (a) Ni-P, and (b) Ni-Fe-P (pH 9.4, temperature 90 °C)

It was speculated that the samples are magnetically soft according to the hysteresis loops. In order to measure the effect of Fe on the magnetic properties of the products, a composite wood veneer with Ni-P alloy was prepared under the same conditions as veneers plated with Ni-Fe-P. It was found that the addition of Fe to the deposits remarkably increased the soft magnetic properties of the products. The saturation magnetization (M_s) of the Ni-Fe-P-coated veneer reached 0.1737 emu, which is higher than the 0.08206 emu of Ni-P coating on *Triplochiton scleroxylon* veneers. Fe can reduce the average magnetic moment of the Ni-Fe-P alloy due to the larger magnetic moments of Fe atoms than those of Ni atoms. Therefore, compared to those of the Ni-P-coated veneers, the ternary Ni-Fe-P alloy-coated veneers had greater magnetic properties.

Corrosion Studies

The corrosion characteristics of plated veneers are shown in Table 2. The polarization resistances (R_p) of the Ni-Fe-P-coated veneers reached 4160.9 Ω , which was higher than the 2866.7 Ω of Ni-P-coated veneers (as shown in Table 2). From a thermodynamic perspective, the greater the electric potential, the stronger the anti-corrosion property tends to be (Hui *et al.* 2013). On the other hand, a low current density indicates good corrosion resistance. Therefore, the anti-corrosion properties of Ni-Fe-P coatings was higher than those of Ni-P coatings.

Table 2. Corrosion Characteristics of Plated Veneers

Sample	E_{corr} (V)	I_{corr} (A)	R_p (Ω)
Ni-P	-0.402	1.43E-05	2866.7
Ni-Fe-P	-0.361	7.89E-06	4160.9

CONCLUSIONS

1. Ni-Fe-P alloys were successfully electroless-plated onto *Triplochiton scleroxylon* wood veneers *via* a simple process.
2. As pH increased from 8.8 to 9.4, the percentage of nickel in the deposits decreased from 93.40 to 92.69 wt.%, the iron content increased from 4.37 to 5.51 wt.%, and the phosphorus content decreased from 2.23 to 1.80 wt.%.
3. Increasing pH favored the co-deposition of nickel and iron. The metal deposition increased and surface resistivity decreased.
4. XRD results indicated that Ni-Fe-P coatings were crystalline within the pH range of 8.8 to 9.6.
5. SEM analysis showed that the nodular shape on coating surface gradually reduced with the increased of pH value.
6. The shielding effectiveness of plated wood veneers reached 45 to 60 dB for frequencies ranging from 9 kHz to 1.5 GHz.
7. Compared to those of Ni-P-coated veneers, Ni-Fe-P-coated veneers had greater magnetic and anti-corrosion properties.

ACKNOWLEDGMENTS

The research was supported by the Fundamental Research Funds for the Central Universities (2572014EB02-01).

REFERENCES CITED

- Al-Saleh, M. H., and Sundararaj, U. (2009). "Electromagnetic interference shielding mechanisms of CNT/polymer composites," *Carbon* 47(7), 1738-1746.
- An, Z. G., Zhang, J. J., and Pan, S. L. (2008). "Fabrication of glass/Ni-Fe-P ternary alloy core/shell composite hollow microspheres through a modified electroless plating process," *Applied Surface Science* 255(5), 2219-2224.
- Gao, C. H. (2005). "Formation mechanism of amorphous Ni-Fe-P alloys by electrodeposition," *Transactions of Nonferrous Metals Society of China* 15(3), 504.
- Hui, B., Li, J., and Wang, L. (2013). "Preparation of EMI shielding and corrosion-resistant composite based on electroless Ni-Cu-P coated wood," *BioResources* 8(4), 6097-6110.
- Hui, B., Li, J., Zhao, Q., Liang, T., and Wang, L. (2014). "Effect of CuSO₄ content in the plating bath on the properties of composites from electroless plating of Ni-Cu-P on birch veneer," *BioResources* 9(2), 2949-2959.
- Kim, B. R., Lee, H. K., Park, S. H., and Kim, H. K. (2011). "Electromagnetic interference shielding characteristics and shielding effectiveness of polyaniline-coated films," *Thin Solid Films* 519(11), 3492-3496.
- Lee, H. C., Kim, J. Y., Noh, C. H., Song, K. Y., and Cho, S. H. (2006). "Selective metal pattern formation and its EMI shielding efficiency," *Applied Surface Science* 252(8), 2665-2672.
- Nagasawa, C., Kumagai, Y., and Urabe, K. (1990). "Electromagnetic shielding effectiveness of particleboard containing nickel-metalized wood-particles in the core," *Journal of Wood Science* 36(7), 531-537.
- Nagasawa, C., Kumagai, Y., and Urabe, K. (1991). "Electroconductivity and electromagnetic-shielding effectiveness of nickel-plated veneer," *Journal of Wood Science* 36(7), 531-537.
- Nagasawa, C., Kumagai, Y., Koshizaki, N., and Kanbe, T. (1992). "Changes in electromagnetic shielding properties of particleboards made of nickel-plated wood particle formed by various pretreatment processes," *Journal of Wood Science* 38(3), 256-263.
- Nagasawa, C., Kumagai, Y., Urabe, K., and Shinagawa, S. (1999). "Electromagnetic shielding particleboard with nickel-plated wood particles," *Journal of Porous Materials* 6(3), 247-254.
- Pang, J., Li, Q., Wang, B., Tao, D., Xu, X., Wang, W., and Zhai, J. (2012). "Preparation and characterization of electroless Ni-Fe-P alloy films on fly ash cenospheres," *Powder Technology* 226, 246-252.
- Wang, L. J., Li, J., and Liu, Y. X. (2005). "Surface characteristics of electroless nickel plated electromagnetic shielding wood veneer," *Journal of Forestry Research* 16(3), 233-236.
- Wang, L. J., Li, J., and Liu, Y. X. (2006a). "Electroless nickel plating on poplar veneer," *Fine Chemicals* 23(3), 230-233.
- Wang, L. J., Li, J., and Liu, Y. X. (2006b). "Preparation of electromagnetic shielding wood-metal composite by electroless nickel plating," *Journal of Forestry Research* 17(1), 53-56.
- Wang, L. J., and Li, J. (2007). "Ultrasound-assisted electroless plating Ni-P alloy on the surface of birch veneer," *Scientia Silvae Sinicae* 43(12), 112-116.

Wang, L. J. and Liu, H. B. (2011). "Electroless nickel plating on chitosan-modified wood veneer," *BioResources* 6(2), 2045-2054.

Wang, L., Zhao, L., Huang, G., Yuan, X., Zhang, B., and Zhang, J. (2000). "Composition, structure and corrosion characteristics of Ni-Fe-P and Ni-Fe-P-B alloy deposits prepared by electroless plating," *Surface and Coatings Technology* 126(2), 272-278.

Article submitted: December 5, 2014; Peer review completed: January 7, 2015; Revised version received and accepted: January 19, 2015; Published: February 2, 2015.